

See discussions, stats, and author profiles for this publication at: <https://www.researchgate.net/publication/266229311>

# The Design Consideration on the Micro Thin Film SOFC

## Article

---

CITATIONS

0

---

READS

10

4 authors, including:



[Q. M. Jonathan Wu](#)

University of Windsor

364 PUBLICATIONS 3,895 CITATIONS

[SEE PROFILE](#)



[Dave Ghosh](#)

National Research Council Canada

38 PUBLICATIONS 1,215 CITATIONS

[SEE PROFILE](#)

Some of the authors of this publication are also working on these related projects:



M.A.Sc Thesis [View project](#)

All content following this page was uploaded by [Q. M. Jonathan Wu](#) on 07 January 2015.

The user has requested enhancement of the downloaded file.

# The Design Consideration on the Micro Thin Film SOFC

Yanghua Tang, Kevin Stanley, Jonathan Wu, and Dave Ghosh  
Institute for Fuel Cell Innovation, National Research Council  
3250 East Mall, Vancouver, B.C. Canada  
E-mail: yanghua.tang@nrc-cnrc.gc.ca

## Abstract

A micro solid oxide fuel cell ( $\mu$ -SOFC) is one possible choice for portable power. Miniaturization of SOFCs can be accomplished by thin film deposition and micromachining. Serious thermal stresses, originating in fabrication and during operation, cause thermomechanical instability of the constituent thin films. The effect of thin film geometry on thermal stress and mechanical stability is evaluated to optimize the structure of thin film. The design of novel thin film structures for SOFCs is presented by using corrugated membranes.

Keywords: micro solid oxide fuel cell, thin film, corrugated membrane, thermal stress.

## 1 Introduction

The architecture of a solid oxide fuel cell consists of a porous anode and cathode, separated by dense solid-oxide electrolyte. The traditional SOFC operates at high temperature where the electrolyte has sufficient ionic conductivity. Since the ionic resistance of the electrolyte decreases with its thickness, the performance can be improved by using a thinner electrolyte. The conventional fabrication of SOFCs is based on bulk ceramic powder process, such as tape casting and screen printing, which don't lend themselves to thin films. With the development of micromachining, it is possible to make dense ceramic thin films with chemical and physical vapour deposition. The schematic structure of micro SOFC with circular thin films is shown in Figure 1.

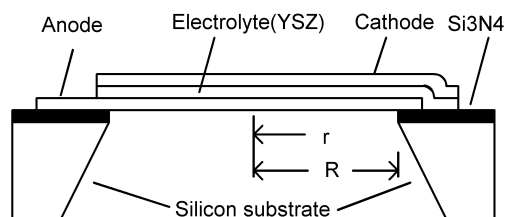


Figure 1: Schematic diagram of thin film SOFC on silicon substrate.

Although the thin film SOFC has the advantage of low temperature ( $300^{\circ}\text{C} \sim 600^{\circ}\text{C}$ ), the surface area of the thin laminated film is limited by the thermal stresses originating in fabrication and during operation. Very small SOFCs increase the number of cells required to reach appreciable power, decreasing efficiency and reliability. Optimization of thin film structures is required to reduce thermal stress, increase the thin film area and improve the cell performance.

## 2 Mechanics of thin film

Layered thin films under thermal loading exhibit several failure modes: buckling, crazing, fracture, and spalling.

Investigation of all failure modes in the layered thin films complicates the design process. Moreover, the key to micro thin film SOFC is to design reliable and dense electrolyte membranes. In the first analysis, a single circular electrolyte membrane is considered. The total stress of microfabricated membrane is the sum of thermal stress, intrinsic stress and external stress. Intrinsic stress can be reduced by modifying the fabrication process parameters and materials. Thus, only thermal stress is analyzed in this paper.

For a flat isotropic membrane with thermal expansion coefficient  $\alpha$  and radius  $R$ , the radial displacement is  $\alpha R \Delta T$  without any constraint at the membrane edge. If the flat membrane is clamped, radial thermal stress  $\sigma_f$  limits the displacement.

$$\sigma_f = -\frac{\alpha E \Delta T}{1 - \nu} \quad (1)$$

where  $E$ , and  $\nu$  are Young's modulus and Poisson ratio of the material respectively.  $E$ ,  $\nu$  and  $\alpha$  of Yttrium stabilized zirconia (YSZ) membrane are 200GPa, 0.2, and  $10 \times 10^{-6} \text{K}^{-1}$  respectively [1]. Negative values of  $\sigma_f$  denote compressive stress. Thermal stress is uniform in the clamped flat membrane and independent on the geometry parameters: membrane thickness  $h$  and radius  $R$ . Thermal expansion of flat membrane is limited everywhere by even thermal stress. But by folding the structure, thermal expansion can be released to some degree and thus the structure stress is reduced.

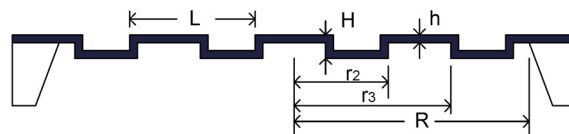


Figure 2: Meridian section of corrugated membrane.

A corrugated membrane used in micromachined sensors can reduce the structure stress by allowing the structure dimension to change. Figure 2 shows the structure of the corrugated membrane. The fundamental parameter of

corrugated membrane is the profile factor  $q$ , which describes the ratio of rigidity of the corrugation. For shallow corrugations in which the ratio of the corrugation depth  $H$  to its wavelength  $L$  is less than 0.4, the profile factor  $q$  is given by [3]

$$q^2 = 1 + 1.5 \frac{H^2}{h^2} \quad (2)$$

$q$  is in the range of 5 to 15 for most corrugated membranes. In special cases, it may be as high as 30. It is 1 for a flat membrane. The radial thermal stress  $\sigma_{cr}$  at radius  $r$  is given by [3]

$$\sigma_{cr} = -\frac{\alpha E \Delta T}{q} \left( \frac{r}{R} \right)^{q-1} \quad (3)$$

Unlike a flat membrane, the radial thermal stress of corrugated membrane is affected by geometry parameters and the maximum thermal stress occurring at the membrane edge.

### 3 Failure criteria

The active surface area of a thin film micro solid oxide fuel cell is an important factor in energy conversion and structure design. Larger surface area leads to higher power output in single cell and simplified stack structure. But a larger surface area ceramic membrane increases the failure rate and reduces the reliability of the materials. So it is necessary to study the relationship between the membrane size and the critical stress. The membrane failure induced by stress is classified by several modes: spalling, fracture, crazing, and buckling. These failure modes are affected by the stress state.

If the membrane tends to expand due to temperature difference, compressive stress occurs. Sufficient compressive stress leads to membrane buckling. For a clamped flat membrane, the critical stress  $\sigma_{fc}$  is given by [7]

$$\sigma_{fc} = -1.22 \frac{E}{1-\nu^2} \left( \frac{h}{R} \right)^2 \quad (4)$$

It is shown that the critical stress is low for thin and large flat membranes, that is when  $h \ll R$ .

Buckling of corrugated membranes occurs when sufficient radial load due to temperature differences between membrane and outer rim is present. The critical stress  $\sigma_{cc}$  is given by

$$\sigma_{cc} = -\frac{E(q+1)^2}{48} \beta^2 \left( \frac{h}{R} \right)^2 \quad (5)$$

where  $\beta$  is the buckling number dependent on  $q$ . For  $q > 10$ ,  $\beta$  changes slightly from 4.8 ~ 5.14 [3]. For the corrugated membrane, it is possible to design large membranes and

keep high critical stress by increasing the profile factor  $q$ . In other words, corrugation with high ratio of  $H:h$  is advantageous.

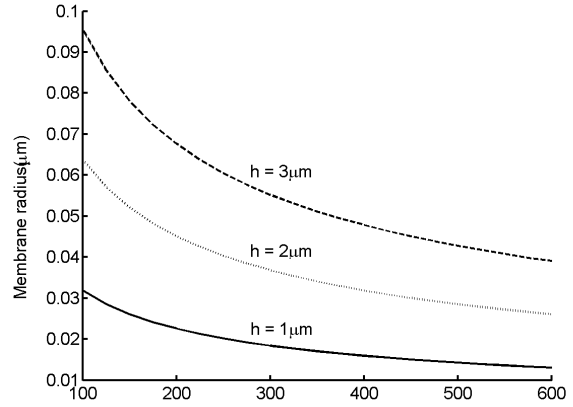


Figure 3 Maximum of the membrane radius versus temperature difference for flat YSZ membrane. ( $E = 200\text{GPa}$ ,  $\nu = 0.2$ ,  $\alpha = 10 \times 10^{-6} \text{K}^{-1}$ )

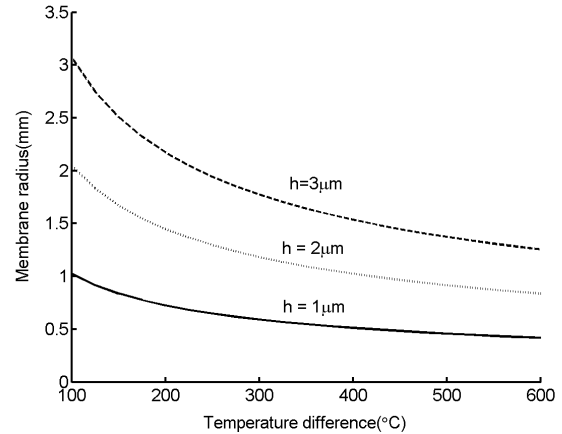


Figure 4: Maximum of the membrane radius versus temperature difference for corrugated YSZ membrane. ( $H:h = 10$ ,  $\beta = 5$ )

Temperature difference  $\Delta T$  as a function of limitation of membrane radius  $R$  in the flat and corrugated membranes is shown in Figure 3 and Figure 4 respectively by combining equation 1 and 4, 3 and 5. It is shown that the maximum radius of the corrugated membrane is substantially greater than that of the flat membrane. For a flat membrane of  $1\mu\text{m}$  thickness, the maximum of the radius is only  $13\mu\text{m}$  at  $\Delta T = 600^\circ\text{C}$ , requiring a large array of cells to obtain sufficient power output. For the  $1\mu\text{m}$ -thick corrugated membrane of  $q = 12$ , the maximum of the membrane radius is  $430\mu\text{m}$  at the same  $\Delta T$ . Corrugation can lead to an order of magnitude increase in cell area for the same temperature.

The main failure mode under the tensile stress is fractures by growth of cracks and flaws. The well-known Weibull statistics can be used to describe fracture failure. This failure model was expanded by Robert Danzer to incorporate the

effects of volumes. For materials containing volume defects, the probability of failure is given by

$$P = 1 - \exp \left[ - \int_{V(\sigma > 0)} n(\sigma) dV \right] \quad (6)$$

Where  $n(\sigma)$  is a material function assumed to be independent on the position in the material and the direction of stress. It is given by

$$n(\sigma) = \frac{1}{V_0} \left( \frac{\sigma}{\sigma_0} \right)^m \quad (7)$$

Where the Weibull modulus  $m$  and stress normalising  $\sigma_0$  are material parameters,  $m$  and  $\sigma_0$  are 6.7 and 236MPa respectively [8].  $V_0$  is an arbitrary normalizing volume and often set to 1 mm<sup>3</sup>. Thermal stress in a flat membrane is isotropic. By integrating  $n(\sigma)$  on a flat circular membrane with radius  $R$  and thickness  $h$ , the failure probability  $P$  is given by

$$P = 1 - \exp \left[ - \frac{2\pi}{V_0} \left( \frac{\sigma_f}{\sigma_0} \right)^m R^2 h \right] \quad (8)$$

The failure probability of a flat membrane increases with the geometry parameter:  $R^2 h$ . Thermal stress in a corrugated membrane is anisotropic. The tangential stress  $\sigma_{ct}$  is given by [3]

$$\sigma_{ct} = -\alpha E \Delta T \left( \frac{r}{R} \right)^{q-1} \quad (9)$$

$n(\sigma)$  is expressed as  $n(\sigma_{cr}) + n(\sigma_{ct})$  in a corrugated membrane. By integrating  $n(\sigma_{cr}) + n(\sigma_{ct})$  over the membrane volume  $V$  in equation 6, the possibility of failure in the rectangular corrugated membrane shown in Figure 2 is given by

$$P = 1 - \exp \left[ - \frac{2\pi}{V_0} (c1 + c2) \left( \frac{\sigma_{cm}}{\sigma_0} \right)^m \right] \quad (10)$$

Where  $\sigma_{cm}$  is the maximum thermal stress in the corrugated membrane:  $\alpha E \Delta T$ ,  $c1$  and  $c2$  are geometry parameters given by

$$c1 = \left( 1 + \frac{1}{q^m} \right) \frac{R^2 h}{m(q-1)+2} \quad (11)$$

$$c2 = \left( 1 + \frac{1}{q^m} \right) h H \sum_{i=1}^{2n} r_i \left( \frac{r_i}{R} \right)^{m(q-1)} \quad (12)$$

Where  $n$  is the corrugation number,  $r_i$  is the radius of the  $i^{th}$  corrugation, as shown Figure 2.  $c1$  is much greater than  $c2$  in a shallow corrugation. The failure probability  $P$  can be simplified by

$$P = 1 - \exp \left[ - \frac{2\pi}{V_0} c1 \left( \frac{\sigma_{fc}}{\sigma_0} \right)^m \right] \quad (13)$$

$c1$  is less than the geometry factor  $R^2 h$  in equation 8 by a factor of  $m(q-1)+2$ . According to equations 8 and 13, it is concluded that the possibility of failure is lower in the corrugated membrane than that in the flat membrane at the same thermal stress. High values of  $q$  can reduce the failure probability of a corrugated membrane.

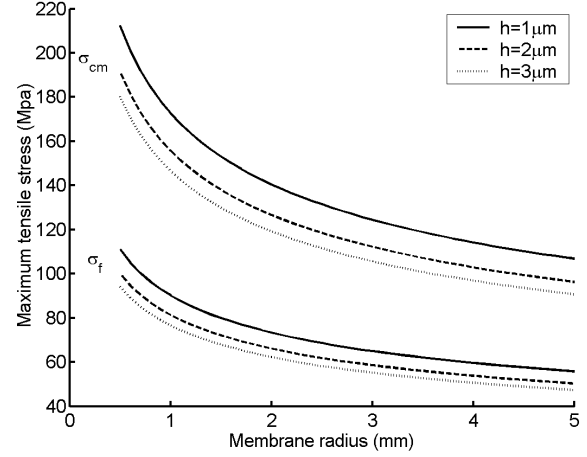


Figure 5: Maximum tensile stress of flat and corrugated membranes versus membrane radius. (For the corrugated membrane,  $n = 5$ ,  $H:h = 10$ )

The critical stress versus membrane radius is plotted in Figure 5 at a failure probability of  $10^{-5}$ . It is shown that critical stress in the corrugated membrane is almost double.

#### 4 Design of membrane structure

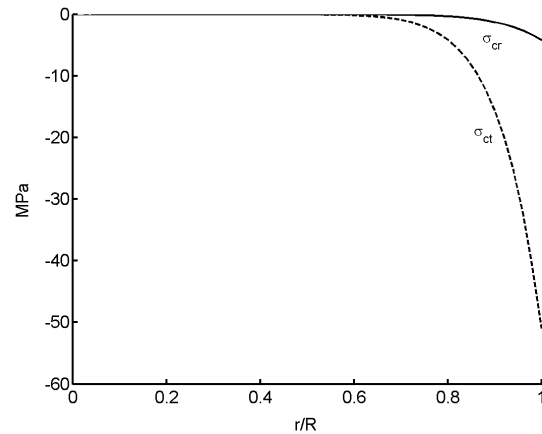


Figure 6: Radius and tangential thermal stress versus relative membrane radius ( $H:h = 10:1$ ).

Compared with the flat membrane, the corrugated membrane has lower thermal stress and higher critical stress. The thermal stress in the corrugated membrane increases by the exponent of the relative radius  $r/R$  and is small in the

middle of the membrane, as shown in Figure 6. The thermal stress occurs only 1.4% at the radius of  $0.7R$  with the corrugation of  $H:h = 10:1$ . The maximum of the thermal stress is at the corrugated membrane edge. The mechanical behaviour of the corrugated membrane can be described as a membrane with a clamped edge and free radial motion. The middle part of corrugated membrane can expand with little constraint and thus very small stress occurs. By making full use of this characteristic, large, thin and flat YSZ films can be mounted on corrugated supported substrates to obtain stable thermomechanical performance, shown in Figure 7. Flat thin films with corrugated edges can expand or contract under temperature variation with little increase in stress. By micromachining, corrugated supported membranes with a large profile factor  $q$  can be fabricated to reduce the stress at the edge. It is feasible to fabricate  $3\mu\text{m}$ -thick YSZ films of 10mm diameter with the corrugated support with  $q$  of 40.

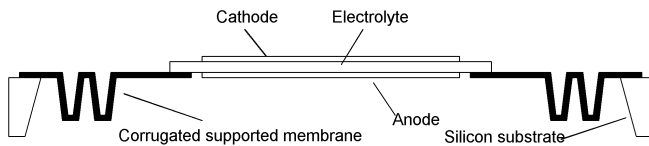


Figure 7: flat thin film of SOFC mounted on corrugated supporting membrane.

## 5 Conclusions

Thermal stress in flat and corrugated film is investigated for micro SOFC. It is shown that lower thermal stress and higher critical stress can be obtained using a corrugated membrane. The radial movement in the corrugated membrane leads to reduced stress in its central area. The membrane mechanical stability is defined by the corrugation profile factor  $q$ .

## References:

1. V.T.Srikar, Kevin T.Turner, Tze Yung Andrew IE, S.Mark Spearing, structural considerations for micromachined solid-oxide fuel cells, *J. Power Sources* 125(2004) 62-69.
2. Robert Danzer, A general strength distribution function for brittle materials, *J. Eu. Ceram. Soc.* 10(1992) 461-472.
3. M. Di Giovanni, Flat and corrugated diaphragm design handbook, Marcel Dekker Inc., New York, 1982.
4. Alan F.Jankowski, Jeffrey P. Hayes, R. Tim Graff, and Jeffrey D. Morse, micro-fabricated thin-film fuel cells for portable power requirements, *Mat.Res.Soc.Symp.Proc.* 730(2002) 93-98.
5. X. Chen, N.J. Wu, L. Smith, and A. Ignatiev, Thin-film heterostructure solid oxide fuel cells, *Applied physics letters*, Vol. 84, No. 14, pp.2700-2702, 2004.
6. Joshua L. Hertz, Jyrki Lappalainen and Harry L. Tuller, Progress towards an all thin film fuel cell for portable power generation, *Electrochemical Society Proceedings*, Vol. 2002-25, pp.137-145.
7. Warren C. Young, *Roark's Formulas for Stress and Strain*, McGraw-Hill Book Company, 1989.
8. C.S. Monstross, H. Yokokawa and M. Dokiya, Thermal stresses in planar solid oxide fuel cells due to thermal expansion difference, *British Ceramic Transactions*, Vol. 101, No. 3, pp.85-93. 2002.